

Structural and electronic analysis of lanthanide complexes: Reactivity may not necessarily be independent of the identity of the lanthanide atom – a DFT study.

Sandra Schinzel¹, Martin Bindl¹, Marc Visseaux² and Henry Chermette^{1}*

¹Laboratoire de Chimie-Physique Théorique, Bât 210 Dirac and CNRS UMR 5182,
Université Claude Bernard Lyon-1, 43 Bd du 11 novembre 1918, 69622 Villeurbanne Cedex,
France,

henry.chermette@univ-lyon1.fr

²Unité de Catalyse et de Chimie du Solide de Lille, UMR 8181 CNRS, ENSCL, Bat C7, Cité
Scientifique, BP 90108, 59652 Villeneuve d'Ascq Cedex, France.

Keywords: lanthanide; rare earth; complexes; catalysis; electronic structure; theory

Received:

Running title: Electronic structure of lanthanide complexes

Abstract

Density functional theory (DFT) calculations were used to study a given complex for the whole series of lanthanide cations: $[\text{Ln}(\text{C}_3\text{H}_5)\text{Cp}(\text{OMe})]$ (1) [$\text{Ln} = \text{La}$ ($Z = 57$) - Lu ($Z = 71$)], the radioactive lanthanide promethium ($Z = 61$) excepted. Contrarily to the common assumptions, the calculations suggest a significant, albeit indirect, contribution of f electrons to bonding. Relativistic effects were considered in the calculations of the bonding energies, as well as in geometry optimisations in both spin-restricted and unrestricted formalisms. The unrestricted orbitals have finally been used for the analysis of the charges and the composition of the frontier orbitals. It is confirmed that the ionic character is more pronounced for complexes of the late lanthanides.

Introduction

In recent years, the chemistry of lanthanides has attracted a great deal of interest, due to their high potential in molecular catalysis.¹⁻⁷

It is commonly assumed that the f electrons of lanthanides are not involved in the chemistry of their complexes, because the f orbitals are significantly more contracted than the valence d or s orbitals in rare earths. This is widely understood because of the dependence of the orbital radii with the principal quantum number, which makes the $4f$ orbitals closer to the nuclei than the $5d$ and further more than the $6s$ orbitals. Moreover, the relativistic effects will contract s and p orbitals with respect to non relativistic ones, and because the nuclei are accordingly more shielded, the f and d orbitals are on the contrary slightly relaxed, leading to destabilized energy levels.^{8,9} Typical orbital radii are given in Table 1.¹⁰

TABLE 1: Orbital radii (pm) of some 4*f*-metals (from ref. (10))

Metal	6s	5d	4f
Ce	217	113	37
Gd	201	102	30
Lu	187	95	25

Because most of the electronic density originating from the *f* orbitals exhibits a rather small overlap with the density of neighbour atoms, taking into account the *f* orbitals into geometry optimization calculations usually leads to geometries quite close to that obtained in calculations where the *f* orbitals are frozen into the so-called pseudopotentials (or effective core potentials), or frozen core approximations. This has been shown at many occasions,^{11–16} and provides a substantial economy in computation power. On the other hand, although the *f* orbitals exhibit a rather small overlap with interacting ligand orbitals, they possess energies which can become rather close to the corresponding ligand ones, and therefore, they can significantly be involved into the reactivity of lanthanide complexes, as already postulated by several authors.^{17–21}

Moreover, the degree of covalency/ionicity in lanthanide-carbon bonds may be related to the catalytic behaviour of rare earths complexes, e.g. for dienes polymerisation,^{22,23} and careful examination of the nature of bonding in active species is therefore of interest, because a slight difference in the ratio may induce significant differences in catalytic properties which respond rather exponentially to energy-related differences. Other properties related to the valence electronic densities may also be affected: in a recent study, Senechal et al. observed a variation of non linear optical (NLO) properties along a series of lanthanide complexes²⁴. NLO properties are known to be sensitive to (valence) electron density localization. Quite recently, Tancrez et al. observed a strong variation of the hyperpolarizability of lanthanide terpyridyl complexes with the *f* orbital filling, suggesting the direct contribution of *f* electrons

to the hyperpolarizability²⁵. In an already old study, Chatterjee et al.²⁶ showed in X-ray diffraction studies that the coordination environment in $\text{Ln}(\text{H}_2\text{O})_9^{3+}$ may vary significantly along the series, and that an excess in charge density located in trans of each ligand could be observed, the maxima being located on a sphere of c.a. 70 pm radius, a value close to 4f orbitals radii (see Table 1).

The purpose of the present paper is to present numerical evidence of this behaviour, which leads to differentiated reactivity of lanthanide complexes with their atomic number, an effect which has often been seen experimentally.^{7,27,28} Therefore, since all rare earths are not equivalent, they have to be carefully selected for new syntheses, taking also into consideration other parameters, like some economical features such as their natural abundance (the lighter ones being the most common ones, and therefore the cheapest).

Computational details

The density functional theory within the Kohn-Sham methodology has been used. Zhang and Wang modified Perdew-Burke-Ernzerhof (PBE) exchange functional (revPBE) coupled to the PBE correlation term have been employed in the generalized gradient approximation (GGA).^{29,30} This functional retains the robustness of PBE and gives improved atomic energies with respect to PBE. The local density approximation (LDA) has been used in a first step for a preliminary geometry optimization of the lanthanum complex. The calculations have been performed using the ADF03 and ADF04 program packages.³¹ When not specified, the basis set is of double- ξ quality (basis II according to ADF02 terminology) and a small frozen core was employed. Therefore the 4f electrons belong to the valence electrons. Relativistic effects are expected to be significant for heavy elements, hence these effects have been taken into account for all electrons in the present calculation with the Zero Order Regular

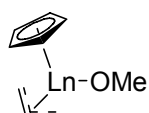
Approximation (ZORA).³²⁻³⁴ Finally the integration grid parameter, setting the numerical integration accuracy, has been fixed to 4.5 or 5.0.

Test calculations have been performed with a larger basis set, namely a triple- ξ + polarization quality (TZP, basis IV in ADF02 terminology) for three complexes, namely those of lanthanum, dysprosium and neodymium. No significant difference with the DZ calculation has been obtained, validating the use of the DZ basis sets for the set of calculations. Supplementary calculations with TZP basis set have also been performed as single points at geometries optimized with the DZ basis set. Finally, bonding energies have also calculated with respect to atoms in open shell state, within a configuration corresponding to the (high spin) ground state, or an average of states of lowest energy. (For the purpose, $C_{\infty v}$ and C_{2v} symmetry have been retained, which do not, however, straightforward lead to f^{5-9} configuration). The spin contamination has been found small in all calculations, the expectation values of $\langle S^2 \rangle$, calculated by the algorithm of Bulow et al.³⁵ deviating only by a few percents above the theoretical value. Detailed validation of the basis set used, and the spin contamination have been collected in supplementary materials section.

All lanthanide complexes have been considered, promethium excepted, because, due to its radioactive-only state, its experimental preparation is more expensive, and no real interest in its chemistry can be found.

Results and Discussion

The studied lanthanide complexes $[\text{Ln}(\text{C}_3\text{H}_5)\text{Cp}(\text{OMe})]$ (**1**) ($\text{Ln} = \text{La} - \text{Lu}$, $\text{Cp} = \text{C}_5\text{H}_5$) (see scheme 1) have three mono-negative ligands.



scheme 1

Therefore, the metal centres are formally at the +3 oxidation state. The Cp ligand, as well as the allyl ligand, are sometimes considered to exhibit a radical-like behaviour in opposition to more ionic ligands (see, e.g. ref. 36). Therefore, if one assigns a minus one half formal charge to each of them, and keeping the methoxy as a single electron acceptor, one obtains a formal charge of +2 for the lanthanide charge. An oxidation degree (O.D.) 2 is still realistic for covalent compounds of lanthanide, whereas the O.D. 3 is known to be traditional in ionic compounds. We will see further on that this formal O.D.= 2 is not far from the theoretical computed charges. Finally, the hapticity of the complex is 9, a value quite common in complexes of elements in the $Z=57$ (La) – $Z=73$ (Ta) range. If the ligands could be considered as points (their centroids), the complex could be regarded as trigonal planar. If we consider more classically that ligands Cp and allyl take 3 and 2 coordination sites, respectively, we have a standard six-fold coordinated complex. This kind of complex was chosen because we wished to consider a potentially reactive molecule. Actually, **1** fits well with this criteria: it bears two moieties, Ln-allyl and Ln-alkoxide, which are known as active species, respectively, towards apolar (e.g. conjugated dienes)³⁷ and polar (e.g. ϵ -caprolactone)³⁸ monomers polymerisation. The stereoelectronic environment is completed by a Cp ligand, and monocyclopentadienyl lanthanide complexes are known to exhibit a catalytic activity towards a large variety of substrates.³⁹ Among the most recent results in the field of lanthanide-based polymerization catalysis, those involving monoCp derivatives are undoubtedly the most spectacular (i.e. the copolymerization of ethylene with dicyclopentadiene⁴⁰, or the insertion of ethylene into syndiotactic sequences of polystyrene⁴¹, and also the refs mentioned in ref.39.)

It is generally accepted that the active moiety in styrene and butadiene (isoprene) coordination polymerization is a metal-allyl one. Actually, a CpLnOR(allyl) molecule

represents a highly probable active species which intervenes in the block copolymerization of styrene with ethylene carried out with a divalent Cp^*LnOAr initiator⁴² (this initiator is oxidized in a trivalent derivative, $\text{Cp}^*\text{LnOAr}(\text{CHPhCH}_2\text{PS})$ -PS is the growing polystyrene chain-, in the presence of styrene). Moreover, it was postulated that the mechanism could exhibit an ionic character, thus it is of interest to evaluate, as done in our study, the nature of bonding in such compounds, especially concerning the active Ln-allyl moiety. As already said, **1**, the molecule under study, is just derived, for evident saving of computational resources, from a $\text{Cp}^*\text{LnOR}(\text{allyl})$ molecule, with Cp instead of Cp^* and OMe instead of OAr.

In a first step, the lanthanum complex $[\text{La}(\text{C}_3\text{H}_5)\text{Cp}(\text{OMe})]$ (**1a**) geometry was optimized by using a medium frozen core and the LDA approximation. (the medium frozen core differs from small frozen core through freezing Ln 5s and 5p orbitals in the medium core). In the great majority of systems, the LDA leads to realistic structures with generally too strong bonds, and sometimes too short distances⁴³. Introducing GGA (gradient-generalized approximation) or most sophisticated exchange-correlation functionals, usually leads to larger bond lengths (and of course more reliable energies), but quasi-homothetic structures. In some cases, however, in particular when weak bonds are present (e.g. explicit solvent molecules), LDA structure may be artefactually distorted⁴⁴. Relativistic effects were not taken into account for this first optimization. In order to check the quality of the basis set, **1a** was recalculated with a small frozen core, so that the 5s and 5p electrons do belong to the valence orbitals. Significantly smaller bond lengths were obtained, indicating that a polarization of the density by the ligands is significant, and needs its description by occupied $s+p+d$ (and f) orbitals. Moreover, the 4f electrons may contribute to the lanthanide complex bonding since the 4f orbital occupation is significantly smaller than its value in a free Ln atom. One can stress that this by no means indicate a direct participation of a f orbital to the bond, but rather

through a non integer occupation (*e.g.* $0.3e^-$ in a Mulliken population analysis of the La complex, see below), a subsequent depletion of the $5d$ orbital, which is more involved in the bonding, is obtained (if one assumes that the $6s$ orbital is quasi-totally depleted in agreement with the oxidation state of the rare earth centre). Therefore the observed effect in the bond length can be considered as an indirect core-valence correlation effect induced by the differences in the (valence) basis set. This effect is similar to that observed by Dolg et al. in their post Hartree-Fock calculation of La and Lu compounds where a significant change in the bond length was found for different size of their active space⁴⁵.

TABLE 2: Bond length (Å) for [La(C₃H₅)Cp(OMe)] (2) computed with the LDA approximation and no relativistic corrections

	d(La-Cn) ^a	d(La-C(1))	d(La-C(2))	d(La-C(3))	d(La-O)	d(O-C(4))
Core medium	2.621	2.766	2.834	2.792	2.141	1.427
Core small	2.555	2.697	2.783	2.740	2.098	1.429

^a Cn is the centroid of the cyclopentadienyl ring

The GGA approximation was employed for further calculations as well as taking into account the relativistic effects within the ZORA formalism. Compared to the previous calculation, for which the LDA approximation and no relativistic effects were used, a significant, but expected,⁴³ bond length increase is obtained (Table 3). It is noteworthy that the values of the bond distances calculated are comprised in the usual ranges for half-metallocenes of the lanthanides: d(Ln-Cp) = ca 2.40-2.60 Å, d(Ln-C(allyl)) = ca 2.60-2.80 Å, d(Ln-O) = ca 2.00-2.1 Å (see for example refs 46, 47)

TABLE 3: Computed (GGA) bond length (Å) for [Ln(C₃H₅)Cp(OMe)] (**1**) [Ln = La - Lu] at the ZORA relativistic level, DZ basis set, small frozen core

	d(Ln-Cn) ^a	d(Ln-C(1))	d(Ln-C(2))	d(Ln-C(3))	d(Ln-O)	d(O-C(4))
La	2.624	2.766	2.831	2.894	2.128	1.459
Ce	2.566	2.718	2.774	2.747	2.105	1.459
Pr	2.559	2.724	2.779	2.742	2.094	1.458
Nd	2.541	2.720	2.764	2.723	2.090	1.456
Sm	2.529	2.772	2.786	2.779	2.085	1.452
Eu	2.521	2.796	2.807	2.880	2.094	1.450
Gd	2.477	2.646	2.685	2.650	2.045	1.452
Tb	2.436	2.634	2.660	2.637	2.041	1.451
Dy	2.444	2.630	2.659	2.635	2.032	1.449
Ho	2.431	2.633	2.653	2.641	2.032	1.447
Er	2.427	2.632	2.665	2.692	2.031	1.446
Tm	2.416	2.684	2.673	2.702	2.032	1.444
Yb	2.405	2.691	2.681	2.807	2.032	1.453
Lu	2.354	2.544	2.566	2.548	1.983	1.445

^a Cn is the centroid of the cyclopentadienyl ring

No strong variation in the bond angles can be noticed, the largest variations being related to:

- i the Cp-Ln-O angle, which increases from 119±1 for La-Sm to 124±1.5 for Gd-Lu,
- ii the central C(allyl)-Ln-O angle, which decreases from 104 for La-Eu to 101±1.5 for Gd-Lu,
- iii the terminal C(Me)-O-Ln angle, which varies from 174 ±1 for La, Ce, and Lu to 178 ±1.5 for others, whereas angles like C-C-C(allyl) remaining constant, equal to 125 ±0.5. The full list of a selection of angles is reported in Table 14 (Supplementary materials)

Variation of the lanthanide center

The heavier the lanthanide atom is, the more important are the relativistic effects. Therefore, the *s* and *p* orbitals of the later lanthanides are more contracted, so that the bond lengths are smaller than for the early lanthanides. This trend known as the "lanthanide contraction" is of course well known and widely described in textbooks⁴⁸. More precisely, the contraction is enhanced by a poor screening effect of the *f* orbitals, an effect which is not additive to the relativistic effect^{49,50}. It has already been observed during the past 10 years, in different contexts, although many calculations were limited to a few Ln atoms of the series^{51,52}. The general trend obtained here is therefore a quasi regular decrease of $d(\text{Ln-Cp})$, $d(\text{Ln-C}_3\text{H}_5)$ and $d(\text{Ln-O})$ when the atomic number of the rare earth increases (Table 3). This regular trend is however broken for $d(\text{Ln-C}_3\text{H}_5)$. The results can be summarized as follows:

For the heavier elements, if one excepts the special cases of Eu and Yb, discussed later, one obtains a quasi-similar Ln-C(1) and Ln-C(3) distance, slightly smaller to Ln-C(2). This is typical to the allyl coordination, the asymmetry Ln-C(1) / Ln-C(3), possibly connected to the absence of symmetry in the complex (because of the methoxy group), being in fact related to a differential localization of the π system (see further).

For the lighter elements, a marked difference, particularly with La, is noticed. This could be tentatively related to the chemical reactivity: it was shown in many occasions that the larger lanthanides (La, Nd) are much more active in conjugated dienes polymerisation^{7,28}. Moreover, in general, allylic molecular catalysts in this series exhibit dissymmetric allylic ligands with one shorter Ln-C distance, like for example $(\text{C}_5\text{Me}_5)\text{Ln}(\text{allyl})_2(\text{dioxane})$ (Ln = La, Nd)⁴³ or similarly in an allyl-neodymium complex for styrene polymerization⁵³ preceding a possible σ - π allylic rearrangement, and hence insertion of the monomer^{54,55}. On the other hand, $\text{Nd}(\text{allyl})\text{Cl}(\text{THF})_5^+$, proved as inactive, bears a symmetric allyl group⁴⁶.

When the series crosses the europium and ytterbium cases, the Ln-allyl bonding involves preferentially Ln-C(1) and Ln-C(2). The splitting up of the two distances Ln-C(1) and Ln-C(3) observed indicates that one external carbon of the allylic group is much less bonded to the central Ln atom than the two other carbons, keeping an enhanced radical character of the allyl. Said differently, the allylic group does not exhibit a so strong delocalization of its π system as in other complexes. In the HOMO -1 of these two complexes, the coefficient of the p orbital for the further of the two outer carbon is bigger than for the closest one (Figure 1).

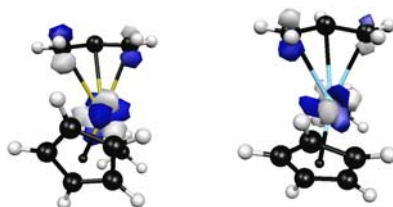


FIGURE 1 : HOMO – 1 of compound **1**, left : Ln = Eu, right: Ln = Yb (the left carbon is the longer bonded one)

TABLE 4 : HOMO – 1 composition for $\text{Ln}(\text{C}_3\text{H}_5)\text{Cp}(\text{OMe})$ (**1**) [Ln = Eu, Yb] and Energy (eV)

	C(1)	C(3)	Ln	Other atoms	Energy
Eu	4.9% p	6.8% p	74.8% f	13.6%	-4.739
Yb	4.3% p	6.4% p	81.4% f	7.9%	-4.818

This is directly connected to the differences in the corresponding bond lengths, reported in Table 3.

Furthermore, the values $d(\text{Ln-Cp})$ and $d(\text{Ln-O})$ are also special for these two elements: e.g. the Eu-O or Eu-Cp is slightly longer than expected from an extrapolation of the corresponding bond lengths for the Ce-Sm complexes. Indeed, one knows that Eu and Yb elements exhibit easily a formal oxidation state of +2 rather than +3, because in such case, they have one half-occupied f shells. This assumption is confirmed by the charge analysis (Table 5). If an atom has a lower oxidation state, its covalent radius is larger, what is found for these two elements. By way of illustration, the Yb-ketyl complex $(\text{C}_5\text{Me}_4\text{SiMe}_2\text{NPh})\text{Yb}(\text{OC}_{13}\text{H}_8)(\text{THF})_2$, in which the Yb element exhibits some divalent character, displays a significantly higher Yb-O distance⁴⁷ (2.15 vs 2.04 Å) than in the pure Yb (III) dimeric $[(\text{C}_5\text{Me}_4\text{SiMe}_2\text{NPh})\text{Yb}(\mu\text{-OC}_{13}\text{H}_8)(\text{THF})]_2$.

The following of the discussion will be related to the atom charges. One knows that they are pure theoretical objects which cannot be measured. However they provide great insight in the chemical properties. The most widely used are Mulliken⁵⁶ charges which can be divided into s, p, d, f subcharges, but which are basis set dependent, and sometimes unrealistic. Hirshfeld⁵⁷ charges, on the contrary are more robust, and often preferred, but less often calculated by quantum chemical softwares. Looking at the Mulliken charges of the lanthanide centre, an increase from La to Lu is observed – except for Eu and Yb for the reasons just mentioned (see above) –, corresponding to a decrease of the Mulliken charge by *ca.* 0.15 e^- below the interpolated charge of the $Z^{+/-1}$ complexes. The ligands are negatively charged. The charge of the oxygen atom decreases in the same way as the charge of the lanthanide centre increases. Hence the bonding La-O has a very strong ionic character with a charge difference larger than 2.5. This ionic character becomes more important for the late lanthanides (Table 5). Such a conclusion could not be drawn from a similar study involving cyclopentadienyl lanthanide complexes.⁵⁸ In a study bearing on a few lanthanide trihalides, Adamo and Maldivi⁵⁹ reached an opposite conclusion, but their compounds were significantly

different to ours, because of a stronger ionic character of the bonds, and a clearly defined formal O.D. +3 of the Ln atom, in contrast to our complex.

The special cases of Eu and Yb already mentioned for the bond lengths, lead also to different charges on some atoms of the complex. The Mulliken charge on the Ln atom is significantly smaller than could be obtained from an extrapolation the charges of the beginning of the La-Sm or the Gd-Tm series. This is directly related to the already mentioned tendency of these elements to accept O.D. = 2 instead of 3. As a consequence, the allyl anion should exhibit a structure closer to that of an allyl radical. The Mulliken population of its C atoms should reflect the point, and this is indeed visible in Table 5 where the sum of the Mulliken charges of the 3 C atoms is decreased (in absolute value) by c.a. 0.10 electron with respect to the charges for the other eleven complexes. Interestingly, the spin densities on the allyl C increases with the number of unpaired α *f* electrons in the first half of Ln (i.e the number of unpaired *f* electrons), and with the number of β electrons in the second half of Ln (i.e the complement to 7 of the number of unpaired *f* electrons): as it will be discussed further, the spin densities on the allyl carbons vary with the number of *f* electrons lying in the same energy band, as is illustrated in Fig. 5. The sign of the spin density indicates an excess of α spin on the carbons for the late Ln, whereas for the early Ln, the opposite is observed (excess of β). As can be also seen in Table 5, the total charge on the allyl carbons decreases as the spin density increases (whatever its sign). Finally, a significant difference in the charges of the terminal C of allyl is only observed for Eu, Er, and Yb complexes

TABLE 5 : Mulliken charge analysis for [Ln(C₃H₅)Cp(OMe)] (1) [Ln = La - Lu]

	Ln	C(1)	C(2)	C(3)	O	C(Cp) _{average}	$\Delta(\text{Ln}-\text{O})^{\text{a}}$	C(1+2+3) ^b	Δq C(1+2+3) ^c	C(1)-C(3) ^d
La	1.900	-0.818	-0.363	-0.827	-0.784	-0.432	2.684	-2.008	0.000	0.0086
Ce	1.905	-0.812	-0.373	-0.829	-0.781	-0.434	2.686	-2.014	-0.003	-0.017
Pr	1.980	-0.831	-0.373	-0.839	-0.786	-0.441	2.766	-2.043	-0.051	-0.0079
Nd	1.938	-0.824	-0.374	-0.827	-0.788	-0.439	2.725	-2.025	-0.124	-0.0009
Sm	1.946	-0.797	-0.391	-0.799	-0.805	-0.443	2.751	-1.987	-0.324	-0.0015
Eu	1.877	-0.742	-0.413	-0.762	-0.825	-0.443	2.702	-1.917	-0.480	-0.0201
Gd	2.158	-0.866	-0.394	-0.866	-0.832	-0.455	2.990	-2.126	-0.010	0.0007
Tb	2.190	-0.842	-0.403	-0.845	-0.836	-0.450	3.026	-2.090	0.010	0.0171
Dy	2.138	-0.857	-0.397	-0.858	-0.841	-0.454	2.979	-2.112	0.091	-0.0004
Ho	2.168	-0.846	-0.406	-0.850	-0.840	-0.458	3.008	-2.102	0.171	-0.0041
Er	2.175	-0.818	-0.412	-0.848	-0.850	-0.461	3.024	-2.078	0.260	0.0298
Tm	2.117	-0.801	-0.422	-0.810	-0.852	-0.461	2.969	-2.033	0.361	0.0089
Yb	2.004	-0.738	-0.438	-0.774	-0.861	-0.455	2.865	-1.950	0.494	0.0355
Lu	2.254	-0.886	-0.404	-0.888	-0.875	-0.460	3.129	-2.178	0.000	-0.0026

^a $\Delta(\text{Ln} - \text{O})$ is the difference of the charges of Ln and O

^b sum of the charges of the allylic carbons

^c sum of the spin densities of the allylic carbons (differences in α and β charges)

^d difference of the charges of the terminal C(1) and c(3) allylic carbons

However, the fact that the oxygen charge and the charge of the external allylic carbons have the same order of magnitude disagrees somewhat with the chemical intuition. Therefore, Hirshfeld charges, often considered as more trustworthy, and more robust against a variation in the basis set^{57,60} are examined. The absolute values of the Hirshfeld charges, reported in Table 6 are smaller than the absolute values of the Mulliken charges. The same conclusion is valid for the charge differences between the Ln atom and the oxygen atom, which represents a measure of the ionic character. Whereas the Mulliken charge analysis indicates an increasing ionic character with Z, the atomic number of the Ln, the Hirshfeld charge analysis, in contrast, does not exhibit such a linear increasing. For the oxygen atom as well as for the metal centre, no uniform developing of the Hirshfeld charge like in the case of the Mulliken charge is observed. Nevertheless, the special attitude for the complexes of Eu and Yb, also observed for the values of the external carbons of the allylic group, is even more visible than in Mulliken analysis, indicating again an increased tendency of the allyl ligand to behave more like an allyl-radical.

TABLE 6 : Hirshfeld charge analysis for [Ln(C₃H₅)Cp(OMe)] (1) [Ln = La - Lu]

	Ln	C(1)	C(2)	C(3)	O	C _{average}	$\Delta(\text{Ln} - \text{O})^a$	C(1+2+3)
La	0.705	-0.184	-0.055	-0.185	-0.342	-0.096	1.047	-0.424
Ce	0.676	-0.177	-0.058	-0.187	-0.330	-0.095	1.007	-0.422
Pr	0.783	-0.190	-0.063	-0.196	-0.365	-0.104	1.149	-0.449
Nd	0.759	-0.185	-0.062	-0.188	-0.361	-0.103	1.121	-0.435
Sm	0.712	-0.164	-0.059	-0.166	-0.364	-0.102	1.076	-0.389
Eu	0.701	-0.140	-0.057	-0.143	-0.379	-0.105	1.080	-0.340
Gd	0.659	-0.181	-0.048	-0.181	-0.333	-0.094	0.992	-0.410
Tb	0.804	-0.193	-0.061	-0.194	-0.371	-0.104	1.175	-0.448
Dy	0.792	-0.190	-0.058	-0.190	-0.374	-0.105	1.166	-0.438
Ho	0.761	-0.180	-0.057	-0.180	-0.368	-0.104	1.129	-0.417
Er	0.748	-0.165	-0.056	-0.176	-0.371	-0.104	1.119	-0.397
Tm	0.736	-0.154	-0.055	-0.157	-0.389	-0.106	1.125	-0.366
Yb	0.716	-0.134	-0.055	-0.138	-0.386	-0.107	1.102	-0.327
Lu	0.669	-0.187	-0.041	-0.188	-0.346	-0.093	1.015	-0.416

^a $\Delta(\text{Ln} - \text{O})$ is the difference of the charges of Ln and O

Finally, the Lu charges show an opposite behaviour within the two charges analysis schemes: Hirshfeld predicts one of the smallest charges, similar to Gd and Ce ones, whereas Mulliken predicts the largest charges of the series. More specifically, the ionic character of the Lu-allyl is one of the largest of the lanthanide series in both schemes, but the Lu-OMe is definitely less ionic in the Hirshfeld scheme, whereas it is more ionic in Mulliken analysis.

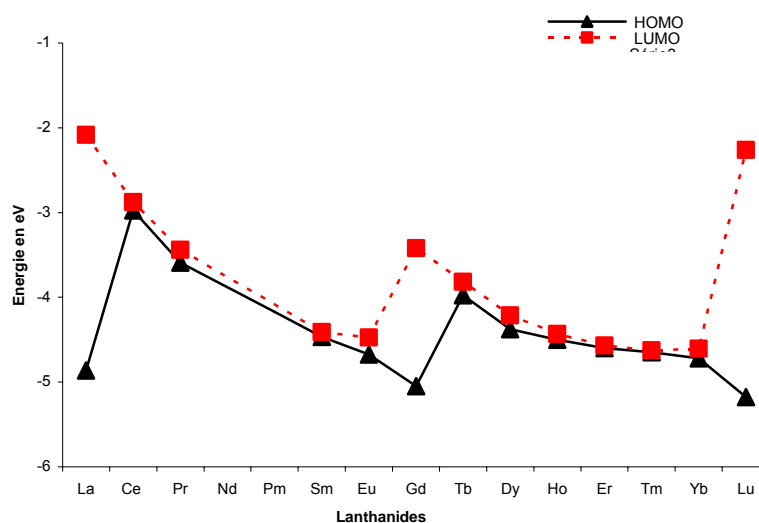


FIGURE 2 : Evolution of the HOMO and LUMO energies within the Ln series

The evolution of the HOMO and the LUMO – defined as the absolute highest HOMO or lowest LUMO of the α and β spinorbitals, whichever comes first – is shown in Figure 2. The energy of the HOMO (LUMO) decreases from Ce to Gd (Eu), then is shifted up and decreases again monotonically up to Lu (Yb) (the energy of the LUMO is higher for Lu, but in that case, it is not an f orbital anymore). The elements with an empty (La), half-occupied (Gd) or completely occupied (Lu) f shell have the greatest HOMO-LUMO gaps and are therefore – according to the maximum hardness principle of Pearson and Parr – the most stable complexes.^{61,66}

In the simplest (closed shell) quantum chemical models, the orbital energy of the frontier occupied orbital(s) varies like the total energy. It is therefore tempting to look at some apparent correlation with the variation of the total energy with the atomic numbers, and the Fig. 2 can be compared to Fig.3.

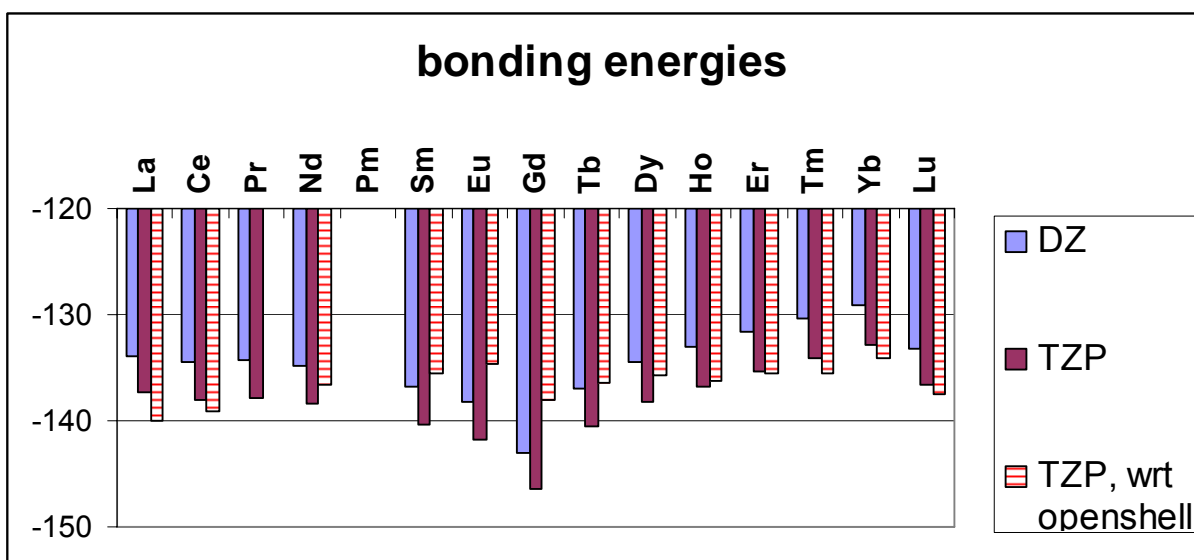


FIGURE 3. Bonding energy variation with the Ln atomic number. DZ, TZP basis sets (with respect to spherical atoms), and (TZP) binding energies with respect to open shell atoms. Energies in eV.

The trend of this graph might be correlated in considering the total energy which decreases continuously as far as Gd. This agrees with the first half of the curve. The diminution of the Coulomb energy due to relativistic effects (shielding) can explain the decrease of the energy in the second half (Table 7). Finally, considering the total energy of these species, this Coulomb energy in the second half is compensated by the kinetic energy which increases if the orbitals are more contracted. A closer look at the kinetic energy shows that it – La and Ce complexes excepted – increases monotonically up to Gd, then is shifted down and increases again. The special behaviour of the two La, Ce complexes is due to the relatively larger occupation of their $5d$ orbital with respect to their $4f$ (Table 8) (let us recall that a $5d$ orbital, which has 2 nodes in its radial function, possesses larger curvatures and therefore larger kinetic energy than a $4f$ orbital which possess no nodes, although being confined in a smaller volume of space). Finally one can notice that these conclusions remain whatever the quality of the basis is used, TZP or DZ, for given geometries optimized at the DZ level of basis set

(the average energy difference between the two basis sets is almost constant, amounting 3.56eV, with a standard deviation as small as 0.10eV).

On the other hand, one should not expect too much from such correlation, because the bonding energies provided by ADF are related to spherical, unrestricted atoms, and along the lanthanide series, the spin polarization varies, enhancing the difference with the atoms within a given spin state. In order to overcome this restriction, bonding energies have also been calculated with respect to open shell atoms, for which the ground state energy has been calculated within the $C_{\infty v}$ or C_{2v} symmetry, leading to definite configurations for most of them. It is interesting to notice that a similar correlation is found, although it is a decrease in the bonding energy which corresponds to an increase of the frontier orbital eigenvalue.

TABLE 7 : Energies (eV) for $[Ln(C_3H_5)Cp(OMe)]$ (1) [$Ln = La - Lu$]. Calculations with the DZ basis set. Total energies in () are calculated with the TZP basis set at geometries optimized with DZ basis sets. Total energies in [] are calculated with the TZP basis set with respect to open shell atoms (at geometries optimized with DZ basis sets).

	HOMO energy	LUMO energy	Electrostatic energy	Kinetic energy	Coulomb energy	XC energy	Total bonding energy, DZ (TZP) [wrt open shell atoms, TZP]
La	-4.862	-2.084	-98.30	107.39	-18.57	-124.36	-133.84 (-137.33)[-109.99]
Ce	-2.976	-2.878	-99.03	103.00	-13.80	-124.69	-134.52 (-138.01) [-109.04]
Pr	-3.592	-3.441	-97.60	45.09	33.54	-115.30	-134.27 (-137.82)
Nd	-4.061	-3.988	-97.55	57.34	22.96	-117.59	-134.85 (-138.45) [-106.58]
Sm	-4.465	-4.410	-96.94	80.36	2.62	-122.89	-136.84 (-140.44) [-105.53]
Eu	-4.674	-4.475	-96.28	92.12	-8.35	-125.72	-138.23 (-141.82) [-104.60]
Gd	-5.047	-3.419	-99.50	127.53	-36.41	-134.69	-143.07 (-146.47) [-108.00]
Tb	-3.975	-3.819	-98.43	68.42	13.97	-120.93	-136.97 (-140.50) [-106.36]
Dy	-4.376	-4.215	-97.99	69.89	12.60	-119.01	-134.52 (-138.20) [-105.79]
Ho	-4.502	-4.432	-98.11	72.73	10.06	-117.76	-133.08 (-136.74) [-106.19]

Er	-4.599	-4.568	-97.73	76.82	5.97	-116.94	-131.59 (-135.28) [-105.47]
Tm	-4.647	-4.627	-97.33	76.43	6.22	-115.66	-130.33 (-134.08) [-105.54]
Yb	-4.721	-4.605	-97.00	80.17	2.77	-115.06	-129.13 (-132.85) [-104.04]
Lu	-5.177	-2.260	-100.87	101.31	-11.25	-122.36	-133.17 (-136.55) [-107.44]

TABLE 8 : Ln Mulliken populations in the valence orbitals for $[\text{Ln}(\text{C}_3\text{H}_5)\text{Cp}(\text{OMe})]$ (1) $[\text{Ln} = \text{La} - \text{Lu}]$, and corresponding spin polarization

	5s+6s		5d		4f		5p		6s+5d+5p	4f	total
Spin	α	β	α	β	α	β	α	β	$\alpha - \beta$	$\alpha - \beta$	$\alpha - \beta$
La	1.035	1.035	0.435	0.435	0.147	0.147	2.934	2.934	0	0	0
Ce	1.034	1.031	0.473	0.410	1.116	0.176	2.931	2.925	0.072	0.940	1.012
Pr	1.033	1.025	0.410	0.361	2.214	0.154	2.917	2.910	0.064	2.060	2.124
Nd	1.042	1.029	0.395	0.335	3.300	0.133	2.920	2.909	0.084	3.167	3.251
Sm	1.033	1.016	0.354	0.266	5.473	0.083	2.914	2.902	0.117	5.390	5.507
Eu	1.036	1.012	0.335	0.251	6.558	0.061	2.940	2.920	0.128	6.497	6.625
Gd	1.038	1.023	0.426	0.320	7.012	0.175	2.936	2.908	0.149	6.837	6.986
Tb	1.070	1.062	0.369	0.290	7.000	1.204	2.922	2.898	0.111	5.796	5.907
Dy	1.041	1.034	0.341	0.271	7.011	2.296	2.946	2.922	0.101	4.715	4.816
Ho	1.027	1.025	0.293	0.240	7.007	3.377	2.941	2.922	0.074	3.630	3.704
Er	1.025	1.025	0.253	0.214	7.003	4.456	2.934	2.916	0.057	2.547	2.604
Tm	1.028	1.029	0.231	0.205	6.998	5.512	2.950	2.930	0.045	1.486	1.531
Yb	1.022	1.023	0.217	0.198	6.994	6.576	2.987	2.978	0.027	0.418	0.445
Lu	1.044	1.044	0.318	0.318	7.011	7.011	3.000	3.000	0	0	0

In general, no striking results are given by the Mulliken population analysis of the valence orbitals: the 5s and the 5p orbitals are almost completely occupied and the filling of the 4f orbitals – at first the orbitals with α -spin up to Gd – follows the general Hund's rule and textbooks chemical laws.

One can notice that the Gd complex with the highest multiplicity (7) is energetically the most stable complex among all the calculated lanthanide ones and it has the greatest exchange-correlation energy (Table 7). This energy increases together with the spin polarization up to Gd (see Table 8, and below), and then it decreases. The spin polarization of the valence shell, 4*f* electrons excepted, increases regularly as the number of unpaired *f* electrons increases, as well as the total spin polarization, although the spin polarization in a 4*f*^{*n*} compound is always significantly larger than in the associated 4*f*^{14-*n*}. Indeed, the excess in spin polarization in a 4*f*^{*n*} compound exceeds that of the 4*f*^{14-*n*} compound by a number of electrons amounting 0.567, 0.593, 0.647, 0.691, and 0.718 for Ce, Pr, Nd, Sm, Eu, respectively. It is interesting to notice that this spin polarization is greater than the number of *f* electrons for the early rare earths (La-Gd), and smaller than the number of holes in the 4*f* shell for the late rare earths (Tb-Lu). This is directly related to the spin polarization of the allylic group reported in Table 5, and the sum of both spin polarizations amounts quite closely the number of *f* electrons (weighting the allylic spin polarization by a factor near 1.2 would indeed further improve the agreement). This feature by itself indicates that the behaviour of all the Ln ions may differ in their interaction with ligand like allyl, the rare earth being not just a spectator. This aspect cannot be evidenced if calculations are performed with frozen cores or pseudo potentials approximations, which do not let the 4*f* electrons relax through the bonding to the ligands.

A look at the frontier orbitals shows that the HOMO of the energetically most stable complexes (La, Gd and Lu) is different from the HOMO of the other lanthanide complexes where the *f* character of the orbitals dominates. For La, Gd and Lu, the *f* orbitals are more stabilized than the *d* orbitals. Therefore, their HOMO is dominated by the *p* orbitals of the allylic carbon and by the *d* orbitals of the lanthanide atom (Figure 4).

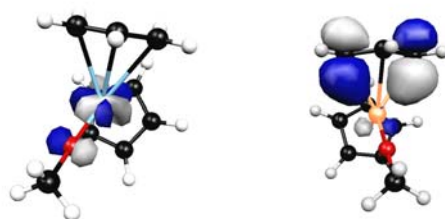


FIGURE 4 : HOMO of compound **1**, left : Ln = Yb, right: Ln = Lu

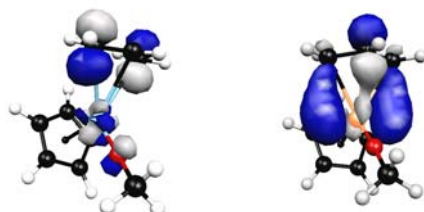


FIGURE 5 : LUMO of compound **1**, left : Ln = Yb, right: Ln = Lu

La and Lu have the same LUMO composition (La $4f$, La $5d$ and p allyl C) (right of Figure 5). But an interesting LUMO composition is observed for Yb and Eu. Here, the LUMO is composed of allylic carbon p orbitals and metal f orbitals (Figure 5 on the left). The LUMOs of the other complexes are almost only pure f orbitals. Going from La to Lu, one can notice that the energy of the HOMO allylic carbon p orbitals does not vary substantially, whereas the $4f$ orbital energies decrease strongly as their atomic number increases.

For La, the allylic carbon $2p$ orbitals have a lower energy than the f orbitals, for Lu it is the reverse. Starting from La, the allylic carbon p orbital penetrates more and more the occupied f orbital band (Figure 6).

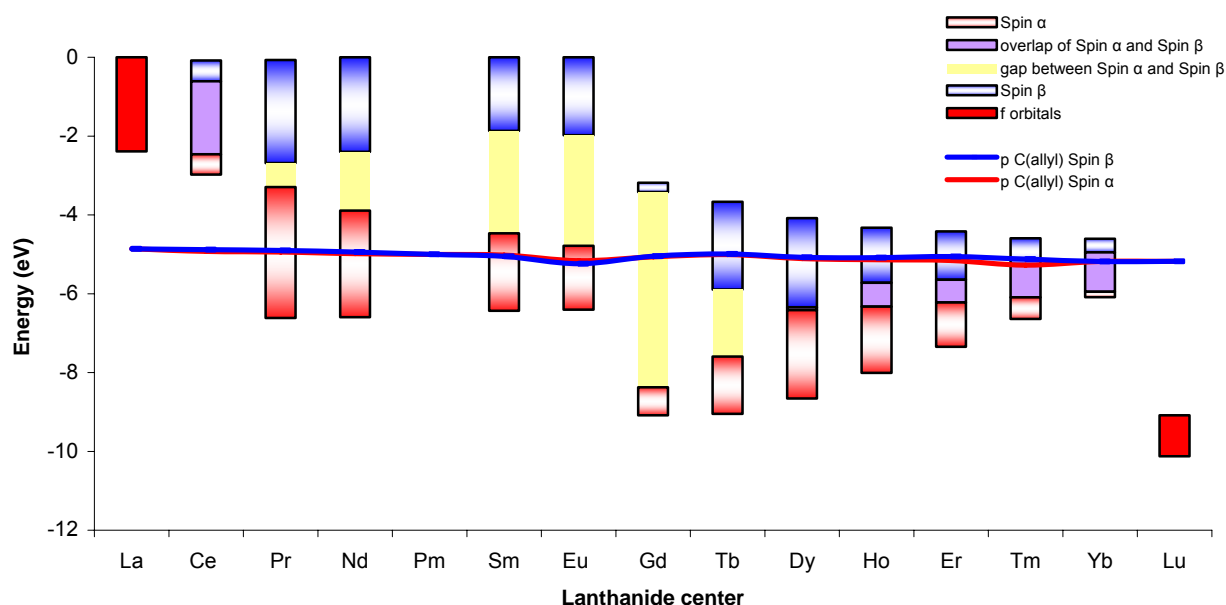


FIGURE 6: Evolution of the f orbital spinorbital energy band with respect to the allyl energy levels along the lanthanide series

As expected, the spin polarization, evaluated as the difference of the orbital energy levels for α spin and β spin is noticed for all open-shell systems. For Ce an overlap of up and down f spinorbital bands is observed. However, for further open-shell elements (Pr to Dy), a gap exists between the f spinorbitals of both spins. This gap is maximal for Gd with the highest multiplicity. Overlap is again found for the complexes of Ho to Yb.

The f orbital bandwidth is very small for Ce and very large for Pr. It becomes smaller up to Gd. Then, it becomes once more larger for Tb and decreases again. Generally, the gap between the $4f$ band and the energetically subsequent orbitals is found rather large, both for the lower energetic and for the higher energetic orbitals.

Conclusion

Theoretical studies of the lanthanide complexes are still difficult, although their number is increasing rapidly. It is shown that, within spin-unrestricted calculations many interesting

results can be obtained, overtaking the geometry optimizations which can provide structures in close agreement with experiment. Various properties like the total energy, the charge distribution within the complexes, as well as the composition and the energy of the frontier orbitals can be calculated, giving insights in potential reactivity of families of complexes.

Contrary to the general opinion, the *f* orbitals are involved in bonding, but this is somewhat an indirect effect: because of the quasi-degeneracy of *4f* and *5d* Ln orbitals within the complexes, the *4f* occupation (or population) may vary and induce a change in the bonding via the *5d* orbital, or to a less extent (because its higher energy) the *6s* orbital (which, on the opposite, has a large possible overlap with ligand orbitals due to their diffuse spatial extension). As it is now well established, relativistic effects are very important for lanthanide complexes. The decrease of the bonding distances from lanthane to lutetium is well described by these effects.

Furthermore, according Hund's rule, the complexes prefer having a half-occupied or an occupied shell. Gadolinium has a half-occupied shell and the multiplicity is the highest, the total energy as well as the corresponding maximal exchange-correlation energy.

Going from the early to the late lanthanides, the spin polarization is less acute, the *f* orbitals become more stable, and less involved in possible reactivity schemes. The difference in the spin polarization within the Ln complexes lets understand differences in catalytic properties, but this feature cannot be seen if frozen cores or pseudo potentials approximations are used in the calculations.

These informative results, which confirm that the reactivity of rare earths complexes cannot be considered as identical through the whole family, should encourage to continuing with detailed analyses of lanthanide complexes.

Acknowledgements. The CINES is acknowledged for a grant of computer time (project cpt2130). Dr. O. Maury is acknowledged for fruitful discussions.

Supporting Information Available: Detailed information on the validation of the model (basis set, spin value). This material is available free of charge via the Internet at <http://pubs.acs.org>.

References and Notes

- (1) Molander, G. A.; Romero, J. A. C. *Chem. Rev.* **2002**, *102*, 2161.
- (2) Kobayashi, S.; Sugiura, M.; Kitagawa, H.; Lam, W. W. L. *Chem. Rev.* **2002**, *102*, 2227.
- (3) Gromada, J.; Carpentier, J. F.; Mortreux, A. *Coord. Chem. Rev.* **2004**, 397.

- (4) Hou, Z.; Wakatsuki, Y. *J. Organomet. Chem.* **2002**, 647, 61.
- (5) Yasuda, H. *J. Pol. Sci. Pol. Chem.* **2001**, 39, 1955.
- (6) Barbier-Baudry, D.; Bonnet, F.; Domenichini, B.; Dormond, A.; Visseaux, M. *J. Organomet. Chem.* **2002**, 647, 167.
- (7) Bonnet, F.; Visseaux, M.; Pereira, A.; Barbier-Baudry, D. *Macromolecules* **2005**, 38, 3162.
- (8) Pyykkö, P. *Chem. Rev.* **1988**, 88, 563.
- (9) Chermette, H.; Hollinger, G.; Pertosa, P. *Chem. Phys. Letters* **1982**, 86, 170.
- (10) WebElementsTM, the periodic table on the WWW, URL: <http://www.webelements.com/Copyright> 1993-2003 Mark Winter [The University of Sheffield and WebElements Ltd, UK].
- (11) Maron, L.; Eisenstein, O.; Alary, F.; Poteau R. *J. Phys. Chem. A* **2002**, 106, 1797.

- (12) Maron, L.; Eisenstein, O. *J. Phys. Chem. A* **2000**, *104*, 7140.
- (13) Maron, L.; Perrin, L.; Eisenstein, O. *J. Chem. Soc. Dalton Trans.* **2002**, 534.
- (14) Perrin, L.; Maron, L.; Eisenstein, O. *Inorg. Chem.* **2002**, *41*, 4355.
- (15) Maron, L.; Perrin, L.; Eisenstein, O. *J. Chem. Soc. Dalton Trans.* **2003**, 4313.
- (16) Poli, R. *Inorg. Chem.* **2003**, *42*, 6682.
- (17) Kaita, S.; Kobayashi, E.; Sakakibara, S.; Aoshima, S.; Furukawa, J. *J. Pol. Sci. Pol. Chem.* **1996**, *34*, 3431.
- (18) Depaoli, G.; Russo, U.; Valle, G.; Grandjean, F.; Williams, A. F.; Long, G. J. *J. Am. Chem. Soc.* **1994**, *116*, 5999.
- (19) Schaverien, C. J. *Adv. Organomet. Chem.* **1994**, *36*, 283.

- (20) Roger, M.; Belkhiri, L.; Thuery, P.; Arliguie, T.; Fourmigué, M.; Boucekkine, A.; Ephritikhine, M. *Organometallics*. **2005**, *24*, 4940.
- (21) Anderson, D.M.; Cloke, F.G.N.; Cox, P.A.; Edelstein, N. M.; Green, J.C.; Pang, T.; Sameh, A.A.; Shalimoff, G. *J. Chem. Soc. Chem. Commun.* **1989**, *46*, 53.
- (22) Zinck, P.; Barbier-Baudry, D.; Loupy, A. *Macromol. Rapid Commun.* **2005**, *26*, 46.
- (23) Arndt, S.; Okuda, J. *Adv. Synth. Catal.* **2005**, *347*, 339.
- (24) Sénéchal, K.; Toupet, L.; Ledoux, I.; Zyss, J.; Le Bozec, H.; Maury, O. *Chem. Commun.* **2004**, 2180.
- (25) Tancrez, N.; Feuvrie, C.; Ledoux, I.; Zyss, J.; Toupet, L.; Le Bozec, H.; Maury, O. *J. Am. Chem. Soc.* **2005**, *127*, 13474.
- (26) Chatterjee, A.; Malsen, E. N.; Watson, K. J. *Acta Cryst.* **1988**, *B44*, 386.
- (27) Jeske, G.; Lauke, H.; Mauermann, H.; Schumann, H.; Marks, T. J. *J. Am. Chem. Soc.* **1985**, *107*, 8111.

(28) Fischbach, A.; Klimpel, M. G.; Widenmeyer, M.; Herdtweck, E.; Scherer, W.; Anwander, R. *Angew. Chem. Int. Ed.* **2004**, *43*, 2234.

(29) Zhang, Y.; Yang, W. *Phys. Rev. Lett.* **1998**, *80*, 890.

(30) Perdew, J. P.; Burke, K.; Ernzerhof, M. *Phys. Rev. Lett.* **1996**, *77*, 3865.

(31a) te Velde G., Bickelhaupt F.M., van Gisbergen S.J.A., Fonseca Guerra C., Baerends E.J., Snijders J.G., Ziegler T. *J. Comput. Chem.* **2001**, *22*, 931.

(31b) Baerends, E.J.; Autschbach, J.; Bérces, A.; Bo, C.; Boerrigter, P.M.; Cavallo, L.; Chong, D.P.; Deng, L.; Dickson, R.M.; Ellis, D.E.; Fan, L.; Fischer, T.H.; Fonseca Guerra, C.; van Gisbergen, S.J.A.; Groeneveld, J.A.; Gritsenko, O.V.; Grüning, M.; Harris, F.E.; van den Hoek, P.; Jacobsen, H.; van Kessel, G.; Kootstra, F.; van Lenthe, E.; McCormack, D.A.; Osinga, V.P.; Patchkovskii, S.; Philipsen, P.H.T.; Post, D.; Pye, C.C.; Ravenek, W.; Ros, P.; Schipper, P.R.T.; Schreckenbach, G.; Snijders, J.G.; Sola, M.; Swart, M.; Swerhone, D.; te Velde, G.; Vernooijs, P.; Versluis, L.; Visser, O.; van Wezenbeek, E.; Wiesenekker, G.; Wolff, S.K.; Woo, T.K.; Ziegler, T. ADF2002.03/ADF2004.01, *SCM; Theoretical Chemistry Vrije Universiteit: Amsterdam, The Netherlands*, <http://www.scm.com>

(32) van Lenthe, E.; Baerends, E. J.; Snijders, J. G. *J. Chem. Phys.* **1993**, *99*, 4597.

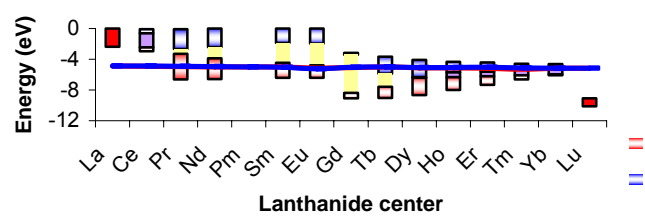
(33) van Lenthe, E.; Baerends, E. J.; Snijders, J. G. *J. Chem. Phys.* **1994**, *101*, 9783.

- (34) van Lenthe, E.; Ehlers, A. E.; Baerends, E. J. *J. Chem. Phys.* **1999**, *110*, 8943.
- (35) Bulo, R.; Ehlers, A. W.; Grimme, S.; Lammertsma, K. *J. Am. Chem. Soc.* **2002**, *124*, 13903, note (29).
- (36) Evans, W.J.; Davis, B. L. *Chem. Rev.* **2002**, *102*, 2119.
- (37) Maiwald, S.; Weissenborn, H.; Sommer, C.; Muller, G.; Taube, R. *J. Organomet. Chem.* **2001**, *640*, 1.
- (38) Barbier-Baudry, D.; Heiner, S.; Kubicki, M. M.; Vigier, E.; Visseaux, M.; Hafid, A. *Organometallics* **2001**, *20*, 4207.
- (39) Arndt, S.; Okuda, J. *Chem. Rev.* **2002**, *102*, 1953.
- (40) Li, X.; Hou, Z. *Macromolecules* **2005**, *38*, 6767.
- (41) Luo, Y. Baldamus, J. Hou, Z. *J. Am. Chem. Soc.* **2004**, *126*, 13910.
- (42) Hou, Z.; Wakatsuki, Y. *J. All. Comp.* **2000** 303-304, 75.

- (43) Chermette, H. *Coord. Chem. Rev.* **1998**, 178-180, 699.
- (44) Gutierrez, F.; Tedeschi, C.; Maron, L.; Daudey, J.P.; Poteau, R.; Azema, J.; Tisnès, J.; Picard, C., *Dalton Trans.*, **2004**, 1334.
- (45) Dolg, M.; Cao, X.-Y., in *Recent Advances in Relativistic Molecular Theory*, Hirao, K., and Ishikawa, Y. ed., World Scientific, Singapore, **2004**, pp. 1.
- (46) Taube, R.; Maiwald, S.; Sieler, J. *J. Organomet. Chem.* **2001**, 621, 327.
- (47) Hou, Z.; Koizumi, T.; Nishiura, M. Wakatsuki, Y. *Organometallics* **2001**, 20, 3323.
- (48) see e.g. Dolg, M., in "Encyclopedia of Computational Chemistry", Vol. 2 (E-L), 'Lanthanides and Actinides', Wiley, Chichester, 1998, p. 1478.; Jensen, F. "Introduction to Computational Chemistry", 1. Auflage, John Wiley & Sons, Chichester 1999.; Miyamoto, T. ; Tsutsui, M., in "*Lanthanide and actinide Chemistry and Spectroscopy*", Edelstein, N.M. ed., ACS, Washington, **1980**, p. 45.
- (49) Bagus, P.; Lee Y.S.; Pitzer, K.S., *Chem. Phys. Lett.* **1975**, 33, 408.

- (50) Seth, M.; Dolg, M.; Fulde, P.; Schwerdtfeger, P., *J. Am. Chem. Soc.* **1995**, *117*, 6597.
- (51) Wang, S. G.; Pan, D. K.; Schwarz, W. H. E. *J. Chem. Phys.* **1995**, *102*, 9296.
- (52) Wang, S. G.; Schwarz, W. H. E., *J. Phys. Chem.* **1995**, *99*, 11967.
- (53) Kirillov, E.; Lehmann, C.W.; Razavi, A.; Carpentier, J-F. *J. Am. Chem. Soc.* **2004**, *126*, 12240.
- (54) Visseaux, M.; Chenal, T.; Roussel, P.; Morteux, A. *J. Organomet. Chem.* **2006**, 691, 86.
- (55) Kaita, S.; Koga, N.; Hou, Z.; Doi, Y.; Wakatsuki, Y. *Organometallics* **2003**, *22*, 3077.
- (56) Mulliken, R. S. *J. Chem. Phys.* **1962**, *36*, 3428.
- (57) Hirshfeld, F. L. *Theor. Chim. Acta* **1977**, *44*, 129.

- (58) Luo, Y.; Selvam, P.; Koyama, M.; Kubo, M.; Miyamoto, A. *Inorg. Chem. Commun.* **2004**, 7, 566.
- (59) Adamo, C.; Maldivi, P., **1998**, *J. Phys. Chem. A* 102, 6812.
- (60) Wiberg, K. B.; Rablen, P.R. *J. Comp. Chem.* **1993**, 14, 1504.
- (61) Chermette H., *J. Comp. Chem.* **1999**, 20, 129.
- (62) Geerlings P., De Proft F., Langenaeker W., *Chem. Rev.* **2003**, 103, 1793.
- (63) Pearson, R.G., *J. Chem. Educ.* **1999**, 76, 267.
- (64) Ayers P.W.; Parr, R.G., *J. Am. Chem. Soc.* **2000**, 122, 2010.
- (65) Pearson, R.G.; *J. Chem. Educ.* **1987**, 64, 561.
- (66) Parr R.G.; Chattaraj, P.K., *J. Am. Chem. Soc.* **1991**, 113, 1854.



TOC graphic:

Supporting information available

(Supplementary material): Validation of the model

a. Quality of the basis set

Taking TZP as a larger basis set, the results do not differ significantly if compared to the afore presented ones calculated with a double- ξ basis (Table 9).

A comparison between the bond lengths shows that the differences in the bond lengths of the complexes calculated with the two (TZP/DZ) basis set are rather small. The d(Ln-O) excepted, all bond lengths are slightly smaller with the larger basis set. The tendency of geometry variation in the lanthanide series remains.

TABLE 9: Computed (GGA) bond length (\AA) for $[\text{Ln}(\text{C}_3\text{H}_5)\text{Cp}(\text{OMe})]$ (1) $[\text{Ln} = \text{La}, \text{Nd}, \text{Dy}]$ using a DZ or a TZP basis set

	d(Ln-Cn) ^a	d(Ln-C(1))	d(Ln-C(2))	d(Ln-C(3))	d(Ln-O)	d(O-C(4))
La DZ	2.624	2.766	2.831	2.894	2.128	1.459
La TZP	2.613	2.767	2.818	2.791	2.152	1.416
Nd DZ	2.541	2.720	2.764	2.723	2.090	1.456
Nd TZP	2.522	2.711	2.748	2.713	2.109	1.413
Dy DZ	2.444	2.630	2.659	2.635	2.032	1.449
Dy TZP	2.421	2.627	2.645	2.626	2.047	1.409

^a Cn is the centroid of the cyclopentadienyl ring

It is known that one drawback of the Mulliken charge analysis is its sensitivity to the basis set. This is clearly the case here. However, a closer look to the charge analysis shows interesting features (Table 10). For the complexes calculated with TZP, the Mulliken charge

is less positive for the metal and less negative for the oxygen atom, indicating a more covalent bond. But the carbons are positively charged and the hydrogens possess a negative charge.

TABLE 10 : Mulliken charge analysis for $[\text{Ln}(\text{C}_3\text{H}_5)\text{Cp}(\text{OMe})]$ (1) $[\text{Ln} = \text{La, Nd, Dy}]$

	Ln	C(1)	C(2)	C(3)	O	C _{average}	$\Delta(\text{Ln-O})^a$
La DZ	1.900	-0.818	-0.363	-0.827	-0.784	-0.432	2.684
La TZP	1.390	0.013	0.258	0.018	-0.649	0.137	2.039
Nd DZ	1.938	-0.824	-0.374	-0.827	-0.788	-0.439	2.725
Nd TZP	1.375	0.012	0.257	0.019	-0.667	0.135	2.042
Dy DZ	2.138	-0.857	-0.397	-0.858	-0.841	-0.454	2.979
Dy TZP	1.319	0.004	0.258	0.006	-0.724	0.134	2.043

^a $\Delta(\text{Ln} - \text{O})$ is the difference of the charges of Ln and O

Fortunately, the Hirshfeld analysis delivers more reliable results (Table 11). The metal charge is similar within both basis sets, and the charges of oxygen and the carbons are a little bit less negative within the TZP basis set.

TABLE 11 : Hirshfeld charge analysis for $[\text{Ln}(\text{C}_3\text{H}_5)\text{Cp}(\text{OMe})]$ (1) $[\text{Ln} = \text{La, Nd, Dy}]$

Ln basis	Ln	C(1)	C(2)	C(3)	O	C _{average}	$\Delta(\text{Ln-O})^a$
La DZ	0.705	-0.184	-0.055	-0.185	-0.342	-0.096	1.047
La TZP	0.676	-0.177	-0.058	-0.187	-0.330	-0.095	1.007
Nd DZ	0.759	-0.185	-0.062	-0.188	-0.361	-0.103	1.121
Nd TZP	0.712	-0.164	-0.059	-0.166	-0.364	-0.102	1.076
Dy DZ	0.792	-0.190	-0.058	-0.190	-0.374	-0.105	1.166
Dy TZP	0.761	-0.180	-0.057	-0.180	-0.368	-0.104	1.129

^a $\Delta(\text{Ln} - \text{O})$ is the difference of the charges of Ln and O

As far as the frontier orbitals are concerned, they possess a comparable composition, but their energy is less negative for the complexes calculated with a TZP basis set (Table 12). The total bonding energy is larger with the TZP basis set, which is in agreement with the shorter bond lengths. We stress, however, that the (ADF) "total bonding energy" changes have to be expected to be large when going from DZ to TZP basis. Indeed the changes come from both of the molecular total energy and of the atoms. These last ones are not true atoms (they can be calculated if bond dissociation energies are of interest), but spherical, "spin-restricted" atoms with fractional orbital occupation (e.g. $f_{xyz}^{3/7}$). These bonding energies related to (unphysical) spherical atoms, are consequently basis set dependent. Therefore the amplitude of the difference in bonding energy within TZP and DZ basis sets is (energetically speaking) meaningless. As mentioned in the paper, true dissociation energies would require the calculation of atoms within a given spin state, and have been approximated by open shell, low symmetry, atomic configurations. The other energies (electrostatic, kinetic, Coulomb, exchange-correlation) are in the same range as DZ.

TABLE 12: Energies (eV) for $[\text{Ln}(\text{C}_3\text{H}_5)\text{Cp}(\text{OMe})]$ (1) $[\text{Ln} = \text{La}, \text{Nd}, \text{Dy}]$ using a DZ

or a TZP basis set

	HOMO energy	LUMO energy	Electrostatic energy	Kinetic energy	Coulomb energy	XC energy	Total bonding energy
La DZ	-4.862	-2.084	-98.30	107.39	-18.57	-124.36	-133.84
La TZP	-4.471	-1.790	-100.31	118.36	-30.00	-125.57	-137.33
Nd DZ	-4.061	-3.988	-97.55	57.34	22.96	-117.59	-134.85
Nd TZP	-3.593	-3.521	-99.98	71.36	8.83	-118.86	-138.45
Dy DZ	-4.376	-4.215	-97.99	69.89	12.60	-119.01	-134.52

Dy TZP -3.854 -3.703 -100.41 85.22 -2.83 -120.35 -138.20

b. Spin contamination

TABLE 13: Expectation value of the spin operator $\langle S^2 \rangle$ of some lanthanide complexes

S^2	La	Pr	Eu	Tm
Exact	0.000	2.000	12.000	2.000
Calculated	0.000	2.022	12.451	2.004

As said in the text, to check the amount of spin contamination in the final result, the expectation values of the spin operator, i.e. $\langle S^2 \rangle$, were calculated for some of the lanthanide complexes (Table 13). The obtained values differ from the theoretical $S(S+1)$ values only by a few percent, therefore the spin contamination is weak.

c. Selected bond angles in the structure

TABLE 14: Bond angles in degrees.

angle	La	Ce	Pr	Nd		Sm	Eu	Gd	Tb	Dy	Ho	Er	Tm	Yb	Lu
Cp-Ln-O	118.8	120.3	121.6	119.6		117.9	121.9	124.2	124.6	123.5	122.5	123.2	122.5	125.6	124.7
Cp-Ln-C(2)	134.0	132.6	133.6	135.1		137.9	132.4	133.0	133.3	135.0	136.0	135.6	135.1	133.8	135.8
C(2)-Ln-O	104.8	103.8	104.4	103.8		104.1	104.8	102.8	102.2	101.5	101.4	100.6	102.4	100.2	99.5
Ln-O-C(4)	173.1	174.6	176.8	177.3		178.3	174.9	174.9	177.9	177.8	178.4	179.6	177.3	177.0	175.1
C(1)-C(2)-C(3)	125.2	124.7	124.9	124.7		125.2	125.5	124.8	124.8	124.6	124.6	124.9	125	125.3	124.4